Proceedings of the Czech–Japanese Seminar in Applied Mathematics 2006
Czech Technical University in Prague, September 14-17, 2006
pp. 62–71

COMPARISON OF SEVERAL FINITE DIFFERENCE SCHEMES FOR MAGNETOHYDRODYNAMICS IN 1D AND 2D

PETR HAVLÍK[1] AND RICHARD LISKA[1]

Abstract. In this paper we present comparison of several finite difference methods for ideal Magnetohydrodynamics (MHD) - the system of conservation laws obtained as extension the Euler equations for ideal gas dynamics by including equations for magnetic field evolution. We compare results of composite Lax-Friedrichs and Lax-Wendroff scheme, central scheme of Nessayahu-Tadmor type, WENO and CWENO scheme. Additionally, results from public freely available packages Nirvana and Flash are compared. 1D Cartesian tests concern smooth periodic problem, Brio-Wu problem and intermediate shock formation problem. From 2D Cartesian tests we briefly present the blast and the fast rotor problem. We are interested also in generalization into cylindrical $r-z$ geometry, where composite and CWENO scheme were developed. We conclude our comparison by presenting results on cylindrical 2D conical z-pinch and MHD jet problem.

Key words. Differential scheme, MHD, WENO, CWENO, Nirvana, Flash, smooth periodic problem, Brio-Wu, intermediate shock formation, rotor, blast, z-pinch, MHD jet.

1. Introduction. The system of ideal MHD equations has in non-dimensional units (i.e. units, where $\mu = 1$) the following form:

$$\frac{\partial \varrho}{\partial t} + \boldsymbol{\nabla} \cdot (\varrho \boldsymbol{v}) = 0, \tag{1.1}$$

$$\frac{\partial (\varrho \boldsymbol{v})}{\partial t} + \boldsymbol{\nabla} \cdot \left(\varrho \boldsymbol{v}\boldsymbol{v}^{\mathrm{T}} + P^{\star} \mathbf{I}^{3\times 3} - \boldsymbol{B}\boldsymbol{B}^{\mathrm{T}} \right) = 0, \tag{1.2}$$

$$\frac{\partial \boldsymbol{B}}{\partial t} + \boldsymbol{\nabla} \cdot (\boldsymbol{v}\boldsymbol{B}^{\mathrm{T}} - \boldsymbol{B}\boldsymbol{v}^{\mathrm{T}}) = 0, \tag{1.3}$$

$$\frac{\partial E}{\partial t} + \boldsymbol{\nabla} \cdot [\boldsymbol{v}\,(E + P^{\star}) - \boldsymbol{B}(\boldsymbol{v} \cdot \boldsymbol{B})] = 0, \tag{1.4}$$

where ϱ is mass density, $\boldsymbol{v}$ is vector of velocity, $\boldsymbol{B}$ is vector of magnetic induction, E is total energy and $P^{\star}$ is sum of thermal and magnetic pressure,

$$P^{\star} = p + \frac{\boldsymbol{B}^2}{2}. \tag{1.5}$$

The hydrodynamic thermal pressure p can be computed from equation of state for ideal gas given by the relation

$$p = (\gamma - 1) \left[E - \frac{1}{2}\varrho \boldsymbol{v}^2 - \frac{1}{2}\boldsymbol{B}^2 \right], \tag{1.6}$$

where γ is ideal gas constant (ratio of specific heats). Symbol $\mathbf{I}^{3\times 3}$ is used for 3×3 unit matrix and $^{\mathrm{T}}$ denotes trans-positioning. The system is coupled with the constraint

$$\boldsymbol{\nabla} \cdot \boldsymbol{B} = 0 \tag{1.7}$$

[1]Czech Technical University in Prague, Faculty of Nuclear Sciences and Physical Engineering.

which follows directly from Maxwell equations. Using equation (1.3) we can verify, that the divergence of magnetic field doesn't change in time, i.e. if the condition (1.7) is satisfied at initial time, it remains valid at any time later. For numerical solutions of the system this is generally not valid and special techniques have to be used to keep zero divergence magnetic field.

2. Cartesian geometry. In this paragraph we shortly describe numerical methods which have been used for comparisons on several 1D and 2D tests in Cartesian geometry. We consider total of four methods - composite, central, WENO and CWENO, and additionally two - Nirvana (version 3, `http://nirvana-code.aip.de`) and Flash (version 2.5, `http://flash.uchicago.edu`) were taken as free-accessible packages on internet. All methods are of finite difference type and all results were computed on rectangular uniform grid. *Composite* scheme [12] performs one Lax-Friedrichs (LF) step after $n-1$ Lax-Wendroff (LW) steps and will be denoted as LWLFn. Dispersive LW itself is second order of accuracy, while diffusive LF and LWLFn only first. *Central* scheme (described with source code in [2]) on staggered grid uses limited piecewise polynomial reconstruction from cell averages. It requires neither Riemann solver nor eigen-decomposition and also avoids dimensional splitting. *WENO* scheme [9] uses convex weighted combination of essentially non-oscillatory schemes on several stencils for space discretization and Runge-Kutta (RK) methods for time integrating. It is fifth order in space and in following text will be denoted as WENO3 in case of RK3 time integration method (TVD) and WENO5 in case of RK4 method (non-TVD). However, WENO requires local eigenvector decomposition which classifies it to one of the slowest scheme in our comparison. Avoiding eigen-decomposition and applying weighted combination directly to the conserved quantities we obtain *CWENO* (Component-wise WENO) scheme. By all methods, after each time step the magnetic field is corrected to satisfy condition (1.7). This is carried out via constrained transport method (details in [6], [16]). Flash [7] uses MUSCL-type limited gradient reconstruction method and for MHD includes only Cartesian geometry. Nirvana implements semi-discrete Godunov-type central scheme method of second order of accuracy, also only in Cartesian geometry.

2.1. Smooth periodic problem in 1D. This problem with exact solution for Euler equations [8] provides an exact solution for the MHD system as well. Existence of smooth analytical solution enables to test numerical order of accuracy of the schemes. It can be easily verified, that density defined as $\varrho(x,t) = 1 + 0.2\sin[\pi(x - tv^x)]$ and other quantities (i.e. velocity- and magnetic-vector and pressure) constant , $\boldsymbol{v}$(x,t) = const., $\boldsymbol{B}$(x,t) = const., p(x,t) = const. is the solution of MHD system (1.1)–(1.4). We treat this solution on interval $x \in [0,1]$ till final time $t = 1$ with periodic boundary conditions and γ parameter set to 1.4. Table 2.1 shows absolute L_1 errors of density for all schemes on grids with 100-1600 cells (which we denote as $L_1(\varrho, N)$, for grid with N cells). Lower part of table contains numerical order of accuracy $NOA(N)$ defined as $\log_2[L_1(\varrho, N)/L_1(\varrho, 2N)]$ for $N = 100, 200, 400, 800$.

As we can expect: composite scheme is first order of accuracy; LW, central, Nirvana and Flash are second order; WENO3 third and CWENO5, WENO5 are fifth order accurate.

2.2. Brio-Wu problem in 1D. The Brio-Wu Riemann problem is classical MHD test problem [4] used in almost all papers numerically treating MHD equations. Here we present only similar results as for previous periodic problem. Table 2.2 shows $L_1(\varrho, N)$ deviations of numerical solution (on meshes with $N = 200, 400, 800$

TABLE 2.1
Convergence for smooth periodic problem – $L_1(\varrho, N)$ errors for $N = 100, 200, 400, 800$ and 1600 and the numerical order of accuracy $NOA(N) = \log_2(L_1(\varrho, N)/L_1(\varrho, 2N))$ for $N = 100, 200, 400$ and 800.

scheme	LWLF12	LW	Central	CWENO5	WENO3	WENO5	Flash	Nirvana3
$L_1(\varrho)$ 100	4.3e-03	1.36e-04	6.44e-04	9.30e-08	2.77e-08	2.28e-08	8.33e-05	2.95e-04
200	2.1e-03	3.42e-05	1.33e-04	2.90e-09	1.32e-09	7.12e-10	1.93e-05	6.99e-05
400	1.0e-03	8.55e-06	2.64e-05	9.05e-11	9.85e-11	2.21e-11	4.47e-06	1.64e-05
800	5.0e-04	2.14e-06	5.18e-06	2.81e-12	1.02e-11	6.77e-13	1.05e-06	3.89e-06
1600	2.5e-04	5.35e-07	1.01e-06	8.60e-14	1.21e-12	2.05e-14	2.51e-07	9.08e-07
$NOA(100)$	1.0	2.0	2.3	5.0	4.4	5.0	2.1	2.1
$NOA(200)$	1.0	2.0	2.3	5.0	3.7	5.0	2.1	2.1
$NOA(400)$	1.0	2.0	2.3	5.0	3.3	5.0	2.1	2.1
$NOA(800)$	1.0	2.0	2.4	5.0	3.1	5.0	2.1	2.1

TABLE 2.2
Convergence for Brio-Wu test problem – $L_1(\varrho, N)$ deviations (N=200,400,800,1600) from Flash solution using 6400 cells and the $NOA(N) = \log_2(L_1(\varrho, N)/L_1(\varrho, 2N))$ for N= 200, 400, 800.

scheme	LWLF12	Central	CWENO3	CWENO5	WENO3	WENO5	Flash	Nirvana3
$L_1(\varrho)$ 200	1.0e-02	1.4e-02	8.6e-03	8.6e-03	7.2e-03	7.2e-03	5.3e-03	9.7e-03
400	6.6e-03	7.6e-03	4.9e-03	4.9e-03	3.9e-03	3.9e-03	2.5e-03	5.5e-03
800	4.2e-03	4.3e-03	2.7e-03	2.7e-03	2.0e-03	2.0e-03	1.4e-03	2.9e-03
1600	2.6e-03	2.1e-03	1.4e-03	1.4e-03	1.0e-03	1.0e-03	6.2e-04	1.5e-03
$NOA(200)$	0.6	0.8	0.8	0.8	0.9	0.9	1.1	0.8
$NOA(400)$	0.7	0.8	0.9	0.9	0.9	0.9	0.9	0.9
$NOA(800)$	0.7	1.0	1.0	1.0	1.0	1.0	1.2	1.0

and 1600) for density from a reference solution. As the reference solution we use Flash solution with 6400 cells. $NOA(N) = \log_2(L_1(\varrho, N)/L_1(\varrho, 2N))$ for $N = 200, 400$ and 800 is presented in Table 2.2 too. As expected, all the numerical methods are first order accurate for this problem involving discontinuous waves.

2.3. Intermediate shock formation in 1D. This test problem [9] shows how intermediate shocks can be formed from continuous waves. Initially, $B^y(x) = 0.5\sin(2\pi x)$ for $x \in [0, 1]$ and all other quantities are computed using relations $dU^1/R_k^1 = dU^2/R_k^2 = \cdots = dU^m/R_k^m$ (generalized Riemann invariants), where U is conserved-quantities vector and R_k are right eigenvectors of the MHD flux Jacobian. Here, superscripts denote components of vectors. All quantities are normalized to $\varrho = 1$, $\boldsymbol{v} = (0, 0, 0)^T$, $B^x = 1$, $B^z = 0$ and $p = 1$ at points where $B^y = 0$. Since we have one-dimensional problem, B^x is constant and v^z, B^z remain zero, only 4 equations need to be solved. Periodic boundary conditions were applied.

Table 2.3 presents L_1 deviations of B^y at three different times $0.25, 0.6$ and 1 on grid with 100, 200, 400, 800 and 1600 cells with respect to reference WENO5 solution on 6400 cells, together with the numerical order of accuracy $NOA(N)$ for $N = 100, 200, 400, 800$. At time $t = 0.25$ (see Fig. 2.1(a)) the solution is smooth and the NOA of all schemes is close to that one presented in Table 2.1 for smooth periodic problem. At time $t = 0.6$ (see Fig. 2.1(b)) two shocks around $x = 0.13$ and $x = 0.63$ are already formed and the NOA decreases rapidly towards one on whole domain $x \in [0, 1]$, while keeping high values on the interval $x \in [0.2, 0.4]$ (shown in Table 2.4) where the solution is still smooth. At time $t = 1.0$ (see Fig. 2.1(c)) the NOA is low both on whole domain $[0, 1]$ even on sub-domain $[0.2, 0.4]$ where B^y is smooth, however the shock has already passed through this region.

TABLE 2.3

Convergence for intermediate shock formation problem at three times $t = 0.25, 0.6, 1$ – $L_1(B^y, N)$ deviations for $N = 100, 200, 400, 800, 1600$ (on $x \in [0, 1]$) from the reference WENO5 solution using 6400 cells and the $NOA(N) = \log_2(L_1(B^y, N)/L_1(B^y, 2N))$ computed from deviations on $x \in [0, 1]$.

scheme	LWLF12	Central	CWENO3	CWENO5	WENO3	WENO5	Flash	Nirvana3
$t = 0.25$								
$L_1(B^y)$ 100	1.8e-03	1.5e-03	8.0e-06	8.2e-06	8.9e-06	9.0e-06	2.8e-04	5.7e-04
200	8.5e-04	3.4e-04	3.4e-07	3.2e-07	4.3e-07	4.0e-07	6.4e-05	1.4e-04
400	3.9e-04	6.8e-05	1.5e-08	9.7e-09	1.8e-08	1.2e-08	1.5e-05	3.2e-05
800	1.9e-04	1.4e-05	1.3e-09	2.8e-10	1.3e-09	3.4e-10	3.3e-06	7.6e-06
1600	9.3e-05	2.8e-06	1.5e-10	8.1e-12	1.5e-10	9.7e-12	7.8e-07	1.8e-06
NOA(100)	1.1	2.1	4.6	4.7	4.4	4.5	2.1	2.1
NOA(200)	1.1	2.3	4.5	5.0	4.6	5.0	2.2	2.1
NOA(400)	1.1	2.3	3.6	5.1	3.8	5.2	2.1	2.1
NOA(800)	1.0	2.3	3.1	5.1	3.1	5.1	2.1	2.1
$t = 0.6$								
$L_1(B^y)$ 100	1.0e-02	1.2e-02	4.4e-03	4.4e-03	4.9e-03	4.9e-03	4.4e-03	7.1e-03
200	5.3e-03	4.8e-03	2.1e-03	2.1e-03	2.3e-03	2.3e-03	2.0e-03	3.0e-03
400	2.7e-03	2.1e-03	9.9e-04	9.9e-04	1.1e-03	1.1e-03	8.7e-04	1.4e-03
800	1.5e-03	9.6e-04	5.0e-04	5.0e-04	5.4e-04	5.3e-04	4.0e-04	6.6e-04
1600	7.4e-04	4.4e-04	2.3e-04	2.3e-04	2.5e-04	2.5e-04	1.8e-04	3.2e-04
NOA(100)	1.0	1.3	1.1	1.1	1.1	1.1	1.1	1.2
NOA(200)	1.0	1.2	1.1	1.1	1.1	1.1	1.2	1.1
NOA(400)	0.9	1.1	1.0	1.0	1.0	1.0	1.1	1.1
NOA(800)	1.0	1.1	1.1	1.1	1.1	1.1	1.2	1.1
$t = 1.0$								
$L_1(B^y)$ 100	1.6e-02	1.6e-02	7.9e-03	7.9e-03	8.9e-03	8.9e-03	5.9e-03	1.0e-02
200	8.0e-03	7.4e-03	3.9e-03	4.1e-03	4.4e-03	4.4e-03	3.1e-03	5.1e-03
400	4.6e-03	3.8e-03	2.1e-03	2.1e-03	2.2e-03	2.2e-03	1.5e-03	2.6e-03
800	2.0e-03	1.5e-03	1.1e-03	1.1e-03	7.4e-04	7.4e-04	4.2e-04	9.2e-04
1600	1.0e-03	7.2e-04	6.9e-04	6.9e-04	3.5e-04	3.5e-04	1.9e-04	4.5e-04
NOA(100)	1.0	1.2	1.0	1.0	1.0	1.0	1.0	1.0
NOA(200)	0.8	1.0	0.9	0.9	1.0	1.0	1.0	1.0
NOA(400)	1.2	1.4	1.0	1.0	1.6	1.6	1.8	1.5
NOA(800)	0.9	1.0	0.6	0.6	1.1	1.1	1.1	1.0

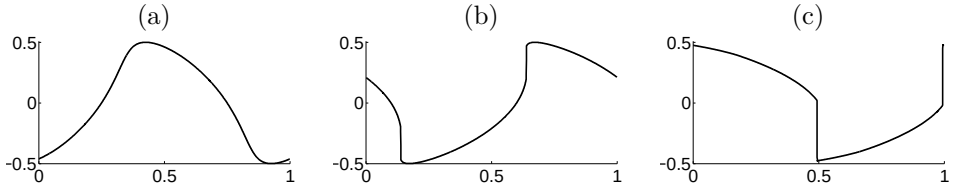

FIG. 2.1. *B^y for intermediate shock formation problem at times $t = 0.25$ (a), 0.6 (b) and 1.0 (c).*

2.4. The Blast problem in 2D. This problem [3] is given on a square $(x, z) \in [-0.5, 0.5] \times [-0.5, 0.5]$ with initial conditions given by

$$\varrho = 1, \quad \boldsymbol{v} = (0, 0, 0)^T, \quad \boldsymbol{B} = (100, 0, 0)^T. \tag{2.1}$$

Pressure p is equal to 1000 for $r \leq 0.1$ and 0.1 otherwise, where we used symbol $r = \sqrt{x^2 + z^2}$ for radius denoting distance from point $(0, 0)$. Ideal gas constant γ was set to 1.4. Fig. 2.2(a) presents magnetic pressure color-map and density contours at time $t = 0.01$ computed by Nirvana code on the mesh with 400×400 cells. 1D cuts along line $x = 0$ for $z \in [-0.45, 0]$ are shown for all schemes in Fig. 2.2(b)-(c),

TABLE 2.4
Convergence for intermediate shock formation problem. Table is similar to Table 2.3 except that $L_1(B^y)$ deviations are computed only on interval $x \in [0.2, 0.4]$.

scheme	LWLF12	Central	CWENO3	CWENO5	WENO3	WENO5	Flash	Nirvana3
$t = 0.6$								
$L_1(B^y)$ 100	7.1e-04	4.5e-04	1.3e-05	1.3e-05	4.3e-05	4.3e-05	3.8e-05	1.6e-04
200	3.0e-04	4.9e-05	1.3e-06	1.3e-06	5.4e-06	5.4e-06	8.1e-06	3.6e-05
400	1.4e-04	9.0e-06	6.2e-08	6.2e-08	4.8e-07	4.8e-07	1.8e-06	7.2e-06
800	6.5e-05	1.2e-06	4.1e-09	4.1e-09	6.4e-09	6.2e-09	5.1e-07	1.5e-06
1600	3.2e-05	2.4e-07	2.2e-10	2.1e-10	2.1e-10	1.9e-10	1.3e-07	3.9e-07
NOA(100)	1.2	3.2	3.4	3.4	3.0	3.0	2.2	2.1
NOA(200)	1.1	2.4	4.4	4.4	3.5	3.5	2.2	2.3
NOA(400)	1.1	2.8	3.9	3.9	6.2	6.3	1.8	2.3
NOA(800)	1.0	2.4	4.2	4.3	4.9	5.0	1.9	2.0
$t = 1.0$								
$L_1(B^y)$ 100	4.9e-04	1.9e-04	1.2e-04	1.2e-04	8.7e-05	8.7e-05	5.6e-05	1.2e-04
200	2.5e-04	7.0e-05	6.1e-05	6.3e-05	4.8e-05	4.8e-05	3.9e-05	6.9e-05
400	1.3e-04	4.9e-05	3.0e-05	3.0e-05	2.6e-05	2.6e-05	2.2e-05	3.4e-05
800	6.7e-05	2.7e-05	1.5e-05	1.5e-05	1.3e-05	1.3e-05	1.1e-05	1.6e-05
1600	3.3e-05	1.3e-05	6.2e-06	6.3e-06	5.7e-06	5.7e-06	4.4e-06	7.0e-06
NOA(100)	1.0	1.4	1.0	1.0	0.9	0.9	0.5	0.8
NOA(200)	1.0	0.5	1.1	1.1	0.9	0.9	0.8	1.0
NOA(400)	0.9	0.9	1.0	1.0	1.0	1.0	1.0	1.1
NOA(800)	1.0	1.1	1.2	1.2	1.2	1.2	1.3	1.2

TABLE 2.5
Execution CPU times of schemes for the fast rotor problem on PC station with Intel Xeon CPU 2.60GHz processor and 2GB operating memory.

scheme	execution time in [hour:]min:sec
LWLF12	13:31
Central	1:39:41
CWENO3	1:34:13
CWENO5	2:13:08
WENO3	3:15:35
WENO5	4:17:00
Flash	15:17
Nirvana3	59:24

where differences between the schemes can be seen. Results are split into two figs with identical axes and one reference solution (Flash).

2.5. The Fast rotor problem in 2D. This is well known, widely published problem, see e.g. [3]. Is was designed as a test for checking torsional Alfven waves propagation. Initial conditions are given on a square $(x, z) \in [-0.5, 0.5] \times [-0.5, 0.5]$ filled by ambient medium with zero velocity in all directions, $\varrho = 1$, $p = 1$ and $\boldsymbol{B} = (5/\sqrt{4\pi}, 0, 0)^T$. At point $(0, 0)$ fast rotating higher density $\varrho = 10$ cylinder (pressure and magnetic field remains constant everywhere) with radius 0.1 is placed having angular velocity 20. The annulus $0.1 \leq r \leq 0.115$ contains smooth pass between cylinder and surrounding medium to avoid sharp discontinuity. The density and velocity in the annulus are given by $\varrho = 70 - 600r$, $v^x = (4000r/3 - 460/3)z$, $v^y = 0$ and $v^z = (-4000r/3 + 460/3)x$, where we used $r = \sqrt{x^2 + z^2}$. Ideal gas constant γ was set to 1.4. On density color-map and contours of magnetic pressure in Fig. 2.2(b) we show results of Nirvana code computed on grid with 340×340 cells at time $t = 0.15$. 1D cuts of magnetic pressure on Fig. 2.2(e)-(f) along line $z = 0$ show profiles of all schemes for $x \in [-0.42, 0]$. We can see more differences of central

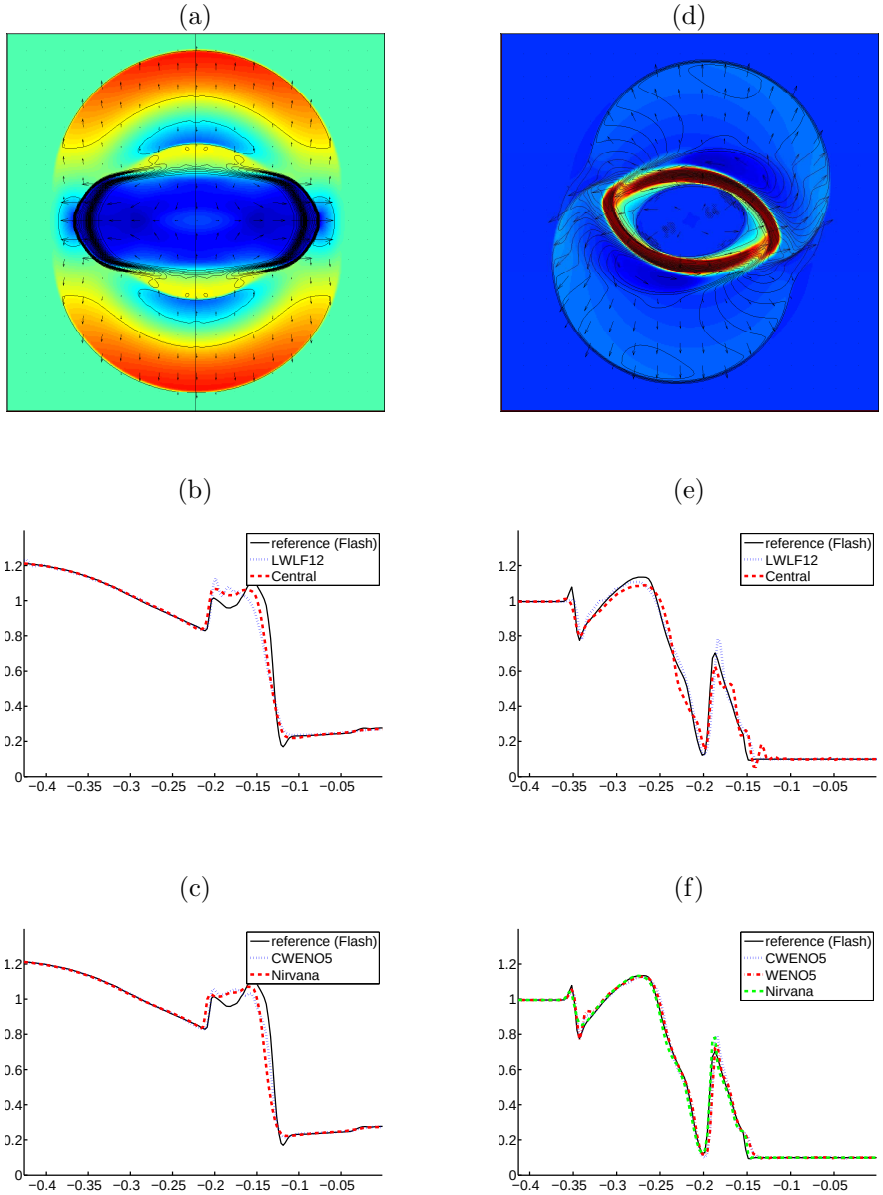

FIG. 2.2. *Magnetic pressure color-map in range* $[190, 663]$ *and 35 density contours in range* $[0.2, 5.3]$ *for blast problem by Nirvana (a); 1D slices in density along line* $x = 0$ *for blast problem (b), (c); density color-map in range* $[0.2, 5.3]$ *and 15 magnetic pressure contours in range* $[0.1, 2]$ *for fast rotor problem by Nirvana (d); 1D slices in magnetic pressure along line* $z = 0$ *for fast rotor problem (e), (f).*

scheme, whereas CWENO5, WENO5 and Nirvana are very close to Flash. Table 2.5 presents comparision of CPU execution times of all schemes. Flash is really very fast, almost four times faster than Nirvana3 and more than eight/seventeen times faster than CWENO5/WENO5. The only faster scheme than Flash is composite LWLF12 but its results are usually fairly worse.

3. Cylindrical geometry. There are no source terms for MHD equations (1.1)–(1.4) in Cartesian geometry, the system is conservative. In cylindrical geometry, the divergence operator $\nabla_{cyl} \equiv (1/r + \partial/\partial r, 1/r\,\partial/\partial\varphi, \partial/\partial z)$ brings source terms into the equations and system is not conservative. Most of these geometric source terms can be included into the fluxes by multiplying the MHD system (except the equation for B^φ) by radius r. Doing that, source terms remain only in two equations for momentum conservation in r and φ directions.

In the first case, if we suppose state variables dependent on r, z and $v^\varphi = B^r = B^z = 0$ at initial (i.e no rotation around z-axis), it can be easy shown, that these variables remain zero later on and thus equations for them can be omitted during computation. System then consists only of 5 equations and only one has source term (eq. for v^r) in the simplest case. This model can be used e.g. for z-pinch simulations (see next paragraph). In general, off course, all variables can be nonzero initially and then we have to solve system of 8 equations. We have developed two methods - composite scheme and CWENO scheme for 2D $r-z$ geometry. Composite scheme has been developed as full 2D predictor-corrector scheme, where both LW and LF schemes use simple averaging to get the source terms on staggered mesh. CWENO scheme has been developed as extension from Cartesian geometry using the same weighted approximation procedure for source terms, that are averaged from the edges midpoints to get the source term inside the cell. Nirvana [17] and Flash [7] support only Cartesian geometry for MHD simulations. Situation with Flash is a little peculiar, because even if we set up the problem in cylindrical geometry, Flash computes in Cartesian geometry without any warning.

3.1. Conical z-pinch in 2D. This test coming from [1] simulates compression of conical z-pinch by magnetic field. Computational domain is rectangular area $(r, z) \in [0, 1.3] \times [0, 1]$ with initial conditions given by values $\varrho = 1$, $\boldsymbol{B} = (0, 0, 0)^T$ for $r \leq 1 + 0.3z$ holds and by values $\varrho = 10^{-4}$, $\boldsymbol{B} = (0, \sqrt{2}/r, 0)^T$ elsewhere. Velocity and pressure are constant in the whole area $\boldsymbol{v} = (0, 0, 0)^T$ and $p = 10^{-4}$. Free boundary conditions on top at $z = 1$ and bottom at $z = 0$ are applied. On right at $r = 1.3$ boundary conditions are free, except Dirichlet boundary conditions for $B^\varphi = \sqrt{2}/r$ for B^φ keeping the tangential magnetic induction. Fig. 3.1 presents density color-map, pressure contours and velocity fields by arrows obtained for this problem by composite (a) and CWENO (b) cylindrical schemes at time $t = 0.63$ on grid with 400×400 cells. Composite scheme is not able to resolve instabilities, seen in CWENO result. Similar instabilities appear also in [1].

3.2. MHD jet problem in 2D. This problem was introduced in [14], other useful texts connected with this subject can be found in [10], [11], [15]. Computational domain of this problem is $(r, z) \in [0, 1] \times [0, 3.32]$, which is initially filled out with ambient medium having zero velocity and magnetic field defined by values $B^r = B^\varphi = 0$ and $B^z = B_{amb} = 0.1$. Sound speed of ambient medium is 1 and ratio of thermal and magnetic pressure (denoted as beta-parameter) is $\beta = 100$. Jet entering the ambient medium at $z = 0$ has radius $r_{jet} = 0.125$, initial Mach number of 20 and ratio of density with respect to ambient medium defined by $\varrho_{jet}/\varrho_{amb} = 0.1$. Jet is in pressure equilibrium with ambient medium and carries helical magnetic field with $B^r = 0$, $B^\varphi = 2B_{amb}r/r_{jet}$ and $B^z = B_{amb}$. The adiabatic index was $\gamma = 5/3$. Boundary conditions are given from geometry as reflective at $r = 0$ and free elsewhere except border at $z = 0$ and $r < r_{jet}$ where the conditions are given by the initial values of the jet. Fig. 3.2 presents density and magnetic pressure for CWENO scheme at four time-shots $t = 0.4, 0.5, 0.6$ and 0.75. Simulation has been done on grid with 256×850

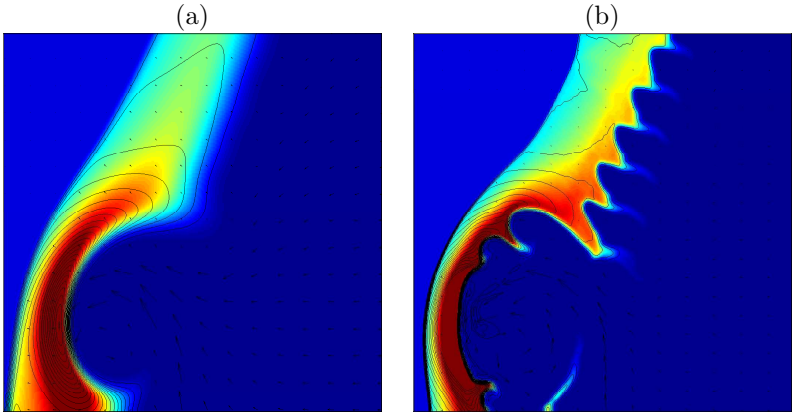

FIG. 3.1. *Density color in range* $[0, 12]$, *25 pressure contours in range* $[0, 26]$ *and velocity field by arrows of LWLF80 (a) and CWENO5 (b) for conical z-pinch in cylindrical geometry.*

cells. We can see similar instabilities as in cited texts. Composite cylindrical scheme was not able to compute this problem.

4. Conclusion. We have presented results of selected finite difference methods in comparison on set of 1D and 2D test problems. Results of low order composite scheme are the worst between others in the sense of resolving discontinuities. Results from high-order CWENO scheme are for most problems very close to WENO scheme. The most precise results in regions of smooth solution are typically obtained by WENO scheme, however it is very slow due to eigenvector decomposition. It seems that in general the best results are produced from Flash code, which is moreover remarkably fast. Nirvana also produces very good results. Composite and CWENO scheme were generalized to cylindrical $r - z$ geometry.

Acknowledgment. This research has been partly supported by the Czech Ministry of Education project MSM 6840770022, research center LC 528, Czech Technical University project CTU0621814 and the Czech Science Foundation project GACR 202/03/H162.

The software Flash used in this work was in part developed by the DOE-supported ASCI / Alliance Center for Astrophysical Thermonuclear Flashes at the University of Chicago.

REFERENCES

[1] A.G. Aksenov, and A.V. Gerusov, *Comparative Analysis of Numerical Methods for 2-Dimensional High Compression MHD Flow Simulation*, Plasma Physics Reports **21**, no. 1 (Jan 1995), 11–19.

[2] J. Balbas, E. Tadmor, and C.-C. Wu, *Non-Oscillatory Central Schemes for One- and Two-Dimensional MHD Equations: I*, J. of Comput. Phys. **201** (2004), 261–285.

[3] D.S. Balsara, and D.S. Spicer, *A Staggered Mesh Algorithm Using High Order Godunov Fluxes to Ensure Selenoidal Magnetic Fields in Magnetohydrodynamic Simulations*, J. of Comput. Phys. **149** (1999), 270–292.

[4] M. Brio, and C.-C. Wu, *An Upwind Differencing Scheme for the Equations of Ideal Magnetohydrodynamics*, J. of Comput. Phys. **75** (1998), 400–422.

[5] W. Dai, and P.R. Woodward, *A Simple Finite Difference Scheme for Multidimensional Magnetohydrodynamical Equations*, J. of Comput. Phys. **142** (1998), 331–369.

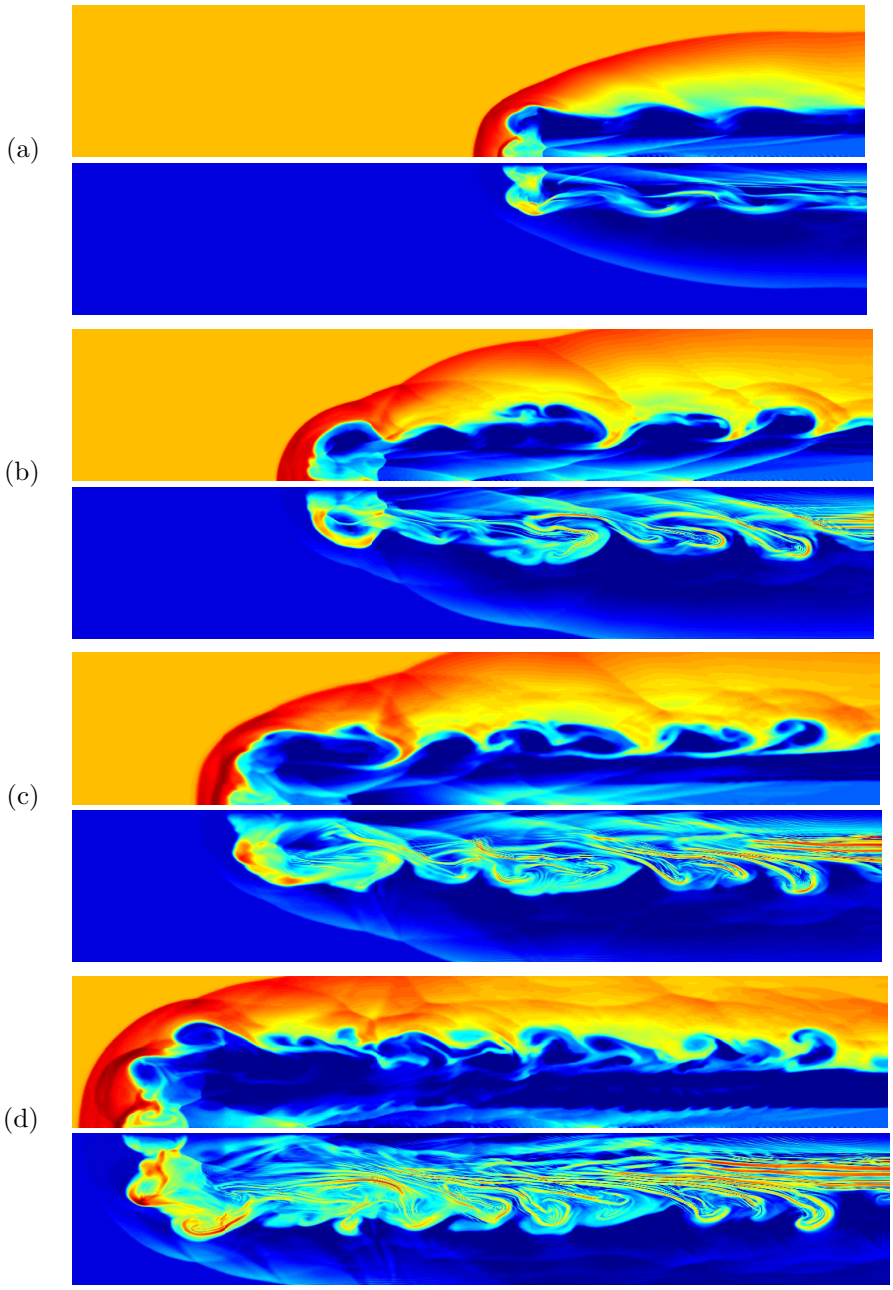

FIG. 3.2. *MHD cylindrical jet problem. Calculations has been done with CWENO scheme on* 250×850 *grid cells with computational domain* $r = [0, 1]$ *and* $z = [0, 3.32]$. *Images show logarithmic density color-map (upper) in range* $[0, 3.8]$ *and logarithmic magnetic pressure color-map (lower) in range* $[0, 2]$ *at* $t = 0.4$ *(a),* 0.5 *(b),* 0.6 *(c) and* 0.75 *(d).*

[6] C.R. Evans, and J.F. Hawley, *Simulation of Magnetohydrodynamic Flows – A Constrained Transport Method*, The Astrophysical J. **332** (1988), 659–677.
[7] ASC FLASH Center, *FLASH user's guide, version 2.3/2.5*, University of Chicago, 2003/2005.
[8] G.S. Jiang, and C.W. Shu, *Efficient Implementation of Weighted ENO Schemes*, J. of Comput. Phys. **126** (1996), 202–228.
[9] G.-S. Jiang, and C.-C. Wu, *A High-Order WENO Finite Difference Scheme for the Equations of Ideal Magnetohydrodynamics*, J. of Comput. Phys. **150** (1999), 561–594.
[10] S. Li, and H. Li, *A Novel Approach of Divergence-Free Reconstruction for Adaptive Mesh Refinement*, J. of Comput. Phys. **199** (2004), 1–15.
[11] K.R. Lind, D.G. Payne, D.L. Meier, and R.D. Blanford, *Numerical Simulation of Magnetized Jets*, The Astrophysical J. **344** (1989), 89–103.
[12] R. Liska, and B. Wendroff, *Composite Schemes for Conservation Laws*, SIAM J. Sci. Comput. **35**, no. 6 (1998), 2250–2271.
[13] P.L. Roe, and D.S. Balsara, *Notes on the Eigensystem of Magnetohydrodynamics*, SIAM J. Appl. Math. **56**, no. 1 (1996), 57–61.
[14] D. Ryu, F. Miniati, T.W. Jones, and A. Frank, *A Divergence-Free Upwinding Code for Multi-Dimensional MHD Flows*, The Astrophysical J. **509** (1998), 244–255.
[15] S. O'sullivan, and T.P. Ray, *Numerical Simulations of Steady State and Pulsed Non-Adiabatic Magnetized Jets from Young Stars*, Astron. Astrophys. **363** (2000), 255–372.
[16] G. Tóth, *The $\nabla \cdot \boldsymbol{B}$ Constraint in Shock-Capturing Magnetohydrodynamics Codes*, J. of Comput. Phys. **161** (2000), 605–652.
[17] U. Ziegler, *A Central-Constrained Transport Scheme for Ideal Magnetohydrodynamics*, J. of Comput. Phys. **196** (2004), 393–416.